

# Numerical simulation of plastic deformation of aluminium workpiece induced by ECAP technology

R. Melicher<sup>a</sup>

<sup>a</sup> Faculty of Applied Mechanics, Žilina university in Žilina, Univerzitná 1, 010 26 Žilina, Slovak Republic

Received 3 September 2009; received in revised form 4 December 2009

---

## Abstract

The objective of this paper was to show some numerical simulations which can be very helpful for optimal settings in extrusion process by equal channel angular pressing (ECAP) technology. Using the finite element (FEM) software ADINA all basic types of used shape of the inner and outer corner of die were modeled. The influence of the tool geometry for plastic strain by simple shear into the aluminum workpiece during extrusion process of the ECAP was analyzed. It was also examined the influence of the pressing force for all usually used variants of die corners.

© 2009 University of West Bohemia. All rights reserved.

*Keywords:* equal channel angular pressing, finite element simulation, accumulative effective plastic strain, effective stress, pressing force

---

## 1. Introduction

In recent years, bulk nanostructured materials (NSM) processed by methods of severe plastic deformation (SPD) have attracted the growing interest of specialists in material science. This interest is conditioned not only by unique physical and mechanical properties inherent to various NSM, e.g. processed by gas condensation or high energy ball milling with subsequent consolidation but also by several advantages of SPD materials as compared to other NSM.

Segal and co-workers developed the method of ECA pressing realizing deformation of massive billets via pure shear in the beginning of 80s. Its goal was to introduce intense plastic strain into materials without changing the cross-section area of billets. Due to that, their repeat deformation is possible. In the early 90s the method was further developed and applied as an (SPD) method for processing of structures with submicron and nanometric grain sizes [1].

Methods of SPD should meet a number of requirements, which are to be taken into account while developing them for formation of nanostructures in bulk samples and billets. These requirements are as follows [1, 2]:

- Firstly, it is important to obtain ultra-fine grained structures with prevailing high angle grain boundaries since only in this case can a qualitative change in properties of materials.
- Secondly, the formation of nanostructures uniform within the whole volume of a sample is necessary for providing stable properties of the processed materials.
- Thirdly, though samples are exposed to large plastic deformations they should not have any mechanical damage or cracks.

---

\*Corresponding author. Tel.: richard.melicher@fstroj.uniza.sk, e-mail: +421 415 132 974.

Traditional methods of SPD, such as rolling, drawing or extrusion cannot meet these requirements. Formation of nanostructures in bulk samples is impossible without application of special mechanical schemes of deformation providing large deformations at relatively low temperatures as well as without determination of optimal regimes of material processing. At present the majority of the obtained results are connected with application of two SPD methods: severe plastic torsion straining under high pressure (SPTS) and equal channel angular pressing (ECAP) [1].

It is well established that SPD is useful for grain refinement in metallic materials. There are so many SPD processes available for grain refinement: for instance, equal channel angular pressing (ECAP), high pressure torsion (HPT), multiple forging and accumulative roll bonding (ARB). A common feature to all these SPD processes is that the cross-sectional dimensions of samples remain unchanged after deformation so that it is possible to introduce large strain into the samples [1, 2].

Of these various procedures, ECAP is an especially attractive processing technique for several reasons:

- First, it can be applied to fairly large billets so that there is the potential for producing materials that may be used in a wide range of structural applications.
- Second, it is a relatively simple procedure that is easily performed on a wide range of alloys and, except only for the construction of the die, processing by ECAP uses equipment that is readily available in most laboratories.
- Third, ECAP may be developed and applied to materials with different crystal structures and to many materials ranging from precipitation-hardened alloys to intermetallics and metal-matrix composites.
- Fourth, reasonable homogeneity is attained through most of the as-pressed billet provided the pressings are continued to a sufficiently high strain.
- Fifth, the process may be scaled-up for the pressing of relatively large samples and there is a potential for developing ECAP for use in commercial metal-processing procedure.

These various attractive features have led to many experimental studies and new developments in ECAP processing over the last decade.

## **2. Fundamental parameters in ECAP**

### *2.1. Slip systems for the different processing routes*

During ECA pressing a billet is multiple pressed through a special die using an ECA facility in which the angle of intersection of two channels is usually  $90^\circ$ . If necessary, in the case of a hard-to-deform material, ECAP is conducted at elevated temperatures.

Since the cross-sectional area remains unchanged, the same sample may be pressed repetitively to attain exceptionally high strain. For example, the use of repetitive pressings provides an opportunity to invoke different slip systems on each consecutive pass by simply rotating the samples in different ways between the various passes [1, 2, 3, 4, 5].

In practice, many of the investigations of ECAP involve the use of bars with square cross-sections and dies having square channels. For these samples, it is convenient to develop processing routes in which the billets are rotated by increments of  $90^\circ$  between each separate pass. The same processing routes are also easily applied when the samples are in the form of rods with the circular cross-sections. During ECAP the direction and number of billet passes through the

channels are very important for microstructure refinement. In papers and books the following routes of billets were considered (see fig. 1) [1, 2, 5]:

- route A where the sample is pressed repetitively without any rotation,
- route  $B_A$  where the sample is rotated by  $90^\circ$  in alternate directions between consecutive passes,
- route  $B_C$  where the sample is rotated in the same sense by  $90^\circ$  between each pass,
- route C where the sample is rotated by  $180^\circ$  between passes.

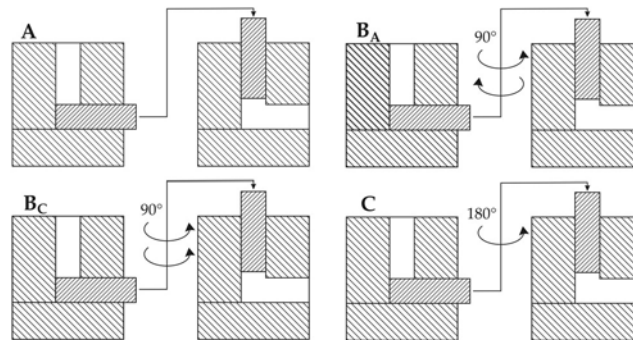


Fig. 1. The four fundamental processing routes in ECAP

The given routes are distinguished in their shear directions at repeat passes of a billet through intersecting channels. Due to that, during ECAP a change in a spherical cell within a billet body occurs.

The different slip systems associated with these various processing routes are depicted schematically in fig. 2 where  $X$ ,  $Y$  and  $Z$  planes correspond to the three orthogonal planes and slip is shown for different passes in each processing route – thus, the planes labelled 1 through 4 correspond to the first 4 passes of ECAP.

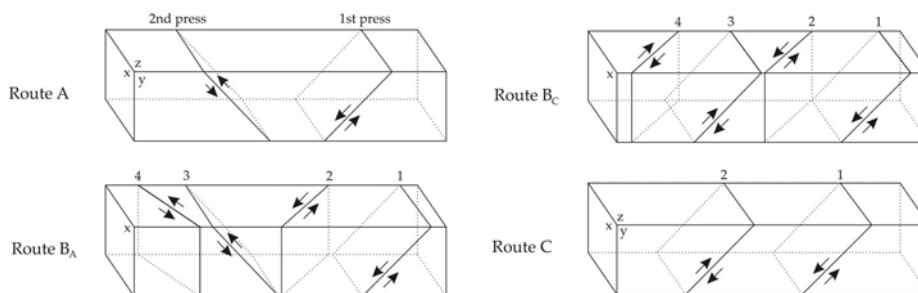


Fig. 2. The slip systems viewed on the  $X$ ,  $Y$  and  $Z$  planes for consecutive passes using processing routes A,  $B_A$ ,  $B_C$  and C

In route C, the shearing continues on the same plane in each consecutive passage through the die but the direction of shear is reversed on each pass – thus, route C is termed a redundant strain process and the strain is restored after every even number of passes. It is apparent that route  $B_C$  is also a redundant strain process because slip in the first pass is cancelled by slip in the third pass and slip in the second pass is cancelled by slip in the fourth pass. By contrast, routes A and  $B_A$  are not redundant strain processes and there are two separate shearing planes intersecting at an angle of  $90^\circ$  in route A and four distinct shearing planes intersecting at angles of  $120^\circ$  in route  $B_A$ . In routes A and  $B_A$ , there is a cumulative build-up of additional strain on each separate pass through the die.

2.2. Analytical solution of the effective plastic strain

Iwahashi et al. have proposed, in 1996, a relation between effective strain  $\varepsilon_{eff}$  and the ECAP angles  $\phi$  (value of the angle within the die between the two parts of the channel) and  $\psi$  (value of the angle at the outer arc of curvature where the channels intersect). This expression is calculated from von Mises isotropic yield criterion applied to the pure shear condition [1, 2]

$$\varepsilon_{eff} = \frac{1}{\sqrt{3}} \left[ 2 \cot \left( \frac{\phi}{2} + \frac{\psi}{2} \right) + \psi \operatorname{cosec} \left( \frac{\phi}{2} + \frac{\psi}{2} \right) \right]. \quad (1)$$

The effective strain  $\varepsilon_{eff}$  in component form is represented by

$$\varepsilon_{eff} = \left[ \frac{2 \left[ \varepsilon_x^2 + \varepsilon_y^2 + \varepsilon_z^2 + \left( (\gamma_{xy}^2 + \gamma_{yz}^2 + \gamma_{zx}^2) / 2 \right) \right]}{3} \right]^{1/2}. \quad (2)$$

Since the same strain is accumulated in each passage through the die, the effective strain after  $N$  extrusion passes  $\varepsilon_N$  may be expressed in a general form by the relationship

$$\varepsilon_N = N \cdot \varepsilon_{eff}. \quad (3)$$

Thus, the strain may be estimated from this equation for any pressing condition provided the angles  $\phi$  and  $\psi$  are known.

2.3. Analytical solution of the extrusion pressure

Alkorta et al. proposed an upper-bound solution to the ECAP pressure considering Hollomon-type materials and using a frictionless condition. According to these authors, the pressure is related with the material hardening behaviour as [1, 2, 5]

$$P = \left( \frac{\sigma_y}{n+1} \right) \left[ \frac{2 \cot \left( (\phi + \psi) / 2 \right) + \psi}{\sqrt{3}} \right]^{(n+1)} \quad (4)$$

where  $\sigma_y$  and  $n$  are yield stress and the strain-hardening exponent, respectively.

An analogue ECAP pressure solution considering a Swift-type material is based on

$$\bar{\sigma} = K (\varepsilon_0 + \bar{\varepsilon}^p)^n \quad (5)$$

where  $K$  is the strength coefficient,  $\varepsilon_0$  is the pre-strain and  $\bar{\varepsilon}^p$  is the effective von Mises plastic strain. Thus, considering one pass of extrusion the equation (4) become

$$P = \left( \frac{K}{n+1} \right) \left\{ \left( \frac{\sigma_y}{K} \right)^{\left( \frac{1}{n} \right)} + \left[ \frac{2 \cot \left( (\phi + \psi) / 2 \right) + \psi}{\sqrt{3}} \right]^{(n+1)} - \left[ \left( \frac{\sigma_y}{K} \right)^{\left( \frac{1}{n} \right)} \right]^{(n+1)} \right\}. \quad (6)$$

The extrusion force per unit of thickness after one pass can be obtained multiplying the right side of the equation (6) by the width ( $W$ ) of the billet. Thus

$$\begin{aligned} \frac{P}{thickness} = W \left( \frac{K}{n+1} \right) & \left\{ \left( \frac{\sigma_y}{K} \right)^{\left( \frac{1}{n} \right)} + \left[ \frac{2 \cot \left( (\phi + \psi) / 2 \right) + \psi}{\sqrt{3}} \right]^{(n+1)} - \right. \\ & \left. - \left[ \left( \frac{\sigma_y}{K} \right)^{\left( \frac{1}{n} \right)} \right]^{(n+1)} \right\}. \end{aligned} \quad (7)$$

### 3. Finite element simulation of ECAP process

Nowadays finite element method is used for simulation of technological processes increasingly. FEM simulations are helpful to estimate some correct parameters of ECAP device and pressing process such as geometry parameters, the pressing speed of the ram, pressing temperature or load displacement curve [1, 2].

#### 3.1. General assumptions in FEM simulation

The FEM is used because it can provide us direct information on the evolution of plastic deformation during the ECAP and enable us to simulate the deformation of materials subjected to single or multi-pass ECAP.

In the FEM simulation, the following assumptions are made [1]:

- First, the material is isotropic and homogeneous.
- Second, the material is elastoplastic with strain-hardening exponent being zero in order to consider the effect of elastic deformation on the morphological change of the extruded billet.
- Third, the system is isothermal.
- Fourth, the von Mises flow rule is used to construct the constitutive relation.
- Fifth, there is no friction between the surface of the material and the die wall due to the use of lubricant in the ECAP.

#### 3.2. FEM formulation of ECAP

It is known that the extruded billet experiences large plastic deformation in the ECAP process. The model based on continuum mechanics needs to allow for arbitrary finite strains.

The elastoplastic behaviour of the billet is described by using a generalization of  $J_2$  flow theory (Prandtl-Reuss equations for isotropic materials with isotropic hardening) to finite strain. In the current configuration  $x_i$ , the components of displacement vector and the metric tensors are denoted as  $u_i$  and  $G_{ij}$ , respectively. In the reference coordinate system  $x^i$ , the components of the displacement vector and the metric tensors are denoted as  $u^i$  and  $g_{ij}$ , respectively. The determinants of  $G_{ij}$  and  $g_{ij}$  are  $G$  and  $g$ , respectively. Then the Lagrangian strain tensor  $\eta_{ij}$  is

$$\eta_{ij} = [(u_{i,j} + u_{j,i}) / 2] + [(u_i^k u_{k,j}) / 2] \quad (8)$$

where  $(\ )_{,j}$  denotes the covariant derivative in the reference frame.

The contravariant components of the Kirchhoff stress  $\tau^{ij}$  and the Cauchy stress tensor  $\sigma^{ij}$  on the current base vectors are related by

$$\tau^{ij} = \sqrt{G/g} \cdot \sigma^{ij}. \quad (9)$$

Using a generalized  $J_2$  flow theory, the tensor of instantaneous moduli  $L^{ijkl}$  relating the stress and strain increments in the constitutive law,  $\dot{\tau}^{ij} = L^{ijkl} \dot{\eta}_{kl}$  is given by

$$L^{ijkl} = \frac{E}{1+\nu} \left[ \frac{1}{2} (G^{ik} G^{jl} + G^{il} G^{jk}) + \frac{\nu}{1-2\nu} G^{ij} G^{kl} - \right. \\ \left. -\alpha \frac{3}{2} \frac{(E/E_t) - 1}{(E/E_t) - (1-2\nu)/3} \frac{s^{ij} s^{kl}}{\sigma_e^2} \right] - \frac{1}{2} [G^{ik} \tau^{jl} + G^{jk} \tau^{il} + G^{il} \tau^{jk} + G^{jl} \tau^{ik}] \quad (10)$$

and

$$\alpha = 1 \text{ if } \dot{\sigma}_e \geq 0 \text{ and } \sigma_e = (\sigma_e)_{\max} \quad \text{or} \quad \alpha = 0 \text{ if } \dot{\sigma}_e < 0 \text{ and } \sigma_e < (\sigma_e)_{\max}$$

here  $E$  and  $\nu$  are Young's modulus and Poisson's ratio, respectively,  $\sigma_e = (3s_{ij}s^{ij}/2)^{1/2}$  is the von Mises stress and  $s^{ij} = \tau^{ij} - (G^{ij}G_{kl}\tau^{kl})/3$  is the stress deviator. The tangent modulus  $E_t$  is the slope of the uniaxial true stress versus logarithmic strain curve at the stress level  $(\sigma_e)_{\max}$ . The curve is represented by a piecewise power law

$$\varepsilon = \begin{cases} \frac{\sigma}{E} & \text{for } \sigma \leq \sigma_y \\ \frac{\sigma_y}{E} \left(\frac{\sigma}{\sigma_y}\right)^{1/n} & \text{for } \sigma > \sigma_y \end{cases} \quad (11)$$

where  $n$  is the strain-hardening exponent and  $\sigma_y$  is the initial yield stress.

For materials without strain-hardening, the deformation is controlled by the criterion,

$$\sigma_e < \sigma_y \quad \text{for elastic deformation,} \quad (12)$$

$$\sigma_e = \sigma_y \quad \text{at yield.} \quad (13)$$

The equivalent plastic strain is defined as

$$\varepsilon^{pl} = \left(\frac{3\varepsilon_{p,ij}\varepsilon_p^{ij}}{2}\right)^{1/2} \quad (14)$$

where  $\varepsilon_{p,ij}$  is the plastic strain tensor.

The equations of equilibrium are defined in terms of the principle of virtual work, which gives

$$\int_V \{\dot{\tau}^{ij}\delta\eta_{ij} + \tau^{ij}\delta\dot{u}_{,i}^k u_{k,j}\} dV = \int_S \dot{T}^i \delta u_i dS - \left[ \int_V \tau^{ij}\delta\eta_{ij} dV - \int_S T^i \delta u_i dS \right] \quad (15)$$

where  $S$  and  $V$  denote the surface and the volume, respectively, in the reference state and  $T^i$  are the contravariant components of the nominal surface tractions. The bracketed terms are included to prevent drifting away from the true equilibrium path.

To simplify the FEM analysis of the ECAP process and increase the computational efficiency, we only analyze two-dimensional problem. Boundary conditions need to be defined to completely determine the deformation behaviour of the billet. Fig. 3 shows the general principle of the ECAP process. The surface of the billet can be divided into six segments ( $S_{AB}$ ,  $S_{BC}$ ,  $S_{CD}$ ,  $S_{DE}$ ,  $S_{EF}$  and  $S_{FA}$ ), depending on the extrusion process.

Considering the use of lubricant in the ECAP, we assume that the contact between the billet and the surfaces of die and punch is frictionless in the FEM simulation. For the segments  $S_{BC}$  and  $S_{EF}$ , there are

$$u_2 = u_0, \sigma^{12} = 0 \text{ and} \quad (16)$$

$$F = \int_{S_{BC}} \sigma^{22} dS \text{ on the segment } S_{BC} \quad (16)$$

$$\sigma^{ij} n_i n_j = 0 \text{ on the segment } S_{EF} \quad (17)$$

where  $n_i$  are the components of the unit normal vector of the segment  $S_{EF}$ .

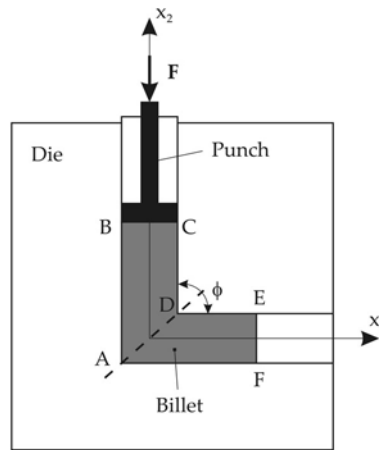


Fig. 3. Schematic diagram of the ECAP process

The boundary conditions for segments  $S_{AB}$ ,  $S_{CD}$ ,  $S_{DE}$  and  $S_{FA}$  involves the inequality equations, which can be expressed as

$$u_1 \geq 0 \text{ and } \sigma^{21} = 0 \text{ on the segment } S_{AB} \quad (18)$$

$$u_1 \leq 0 \text{ and } \sigma^{21} = 0 \text{ on the segment } S_{CD} \quad (19)$$

$$u_i n^i \leq 0 \text{ and } \sigma^{ij} n_i n_j = 0 \quad (i \neq j) \text{ on the segment } S_{DE} \quad (20)$$

$$u_i n^i \geq 0 \text{ and } \sigma^{ij} n_i n_j = 0 \quad (i \neq j) \text{ on the segment } S_{FA} \quad (21)$$

where  $n^i = n_i$ . The inequality indicates that the billet cannot penetrate onto the surface of the die, while separation of the billet from the die can occur.

#### 4. Used finite element models and simulation parameters

The mechanical response of an elastoplastic billet and the deformation behaviour of ECAP process using the commercial FEM software ADINA were made. It was analyzed influence of shape of the inner and outer corner of die.

Very important factor in FEM simulations of forming processes is to find the suitable combination of the mesh density and suitable choice of element type. In these cases occur large deformations – large displacements and large strains. Furthermore, formed bodies are in contact condition with dies or tools during forming process. It means that chosen type of finite elements must fully satisfy contact and deformation conditions and size of the mesh fineness must secure that there will not be too much distortion in these elements during whole simulation. In FEM simulation three nodes linear plane strain elements were used. All FEM simulations were carried out with the same geometry of workpiece and finite element mesh. The two-dimensional workpiece considered has the dimensions of 10 mm (width)  $\times$  50 mm (length) and a unity thickness since a plane strain condition is assumed. The workpiece consisted of 18 426 triangular elements.

The deformation behaviour of Al material workpiece during extrusion process of ECAP was simulated and analyzed. The extrusion of the Al material billet was made by assuming isothermal conditions at room temperature ( $T = 20^\circ$ ) and neglecting the heating conditions due to the friction between the workpiece and the die tool. The details around geometry and main parameters of used FEM models are listed in tab. 1.

Table 1. List of the name and basic parameters of used FEM mode

Name of model	$\phi$	$\psi$	Inner corner radius [mm]
m01	90°	0°	–
m02	90°	90°	–
m03	90°	90°	0,1× width
m04	90°	90°	0,2× width
m05	90°	90°	0,3× width
m06	90°	90°	0,4× width
m07	90°	90°	0,5× width
m08	90°	90°	0,6× width
m09	90°	90°	0,7× width
m10	90°	90°	0,8× width
m11	90°	90°	0,9× width
m12	90°	90°	1,0× width

For this purpose 2D models were developed using a plane strain condition. The coefficient of friction between the inside of the die channel and the workpiece was assumed to be zero implying a frictionless condition. A constant pressing speed of  $1 \text{ mms}^{-1}$  was imposed in each simulation. This constant movement was secured through the displacement function. Workpiece model contained 24 points. Moreover, all points were organized into the four cutting planes and six levels together. These cutting planes and levels can be seen in fig. 4.

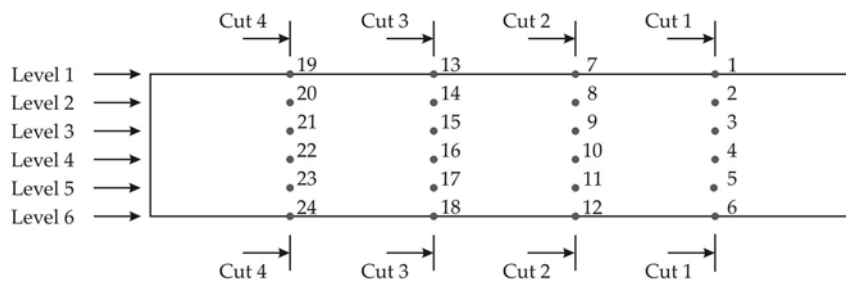


Fig. 4. Analyzed points, cut planes and levels in the workpiece

In general, three combinations of the inner and outer corner shapes are used in practice. Fig. 5 shows these the most widely used variants.

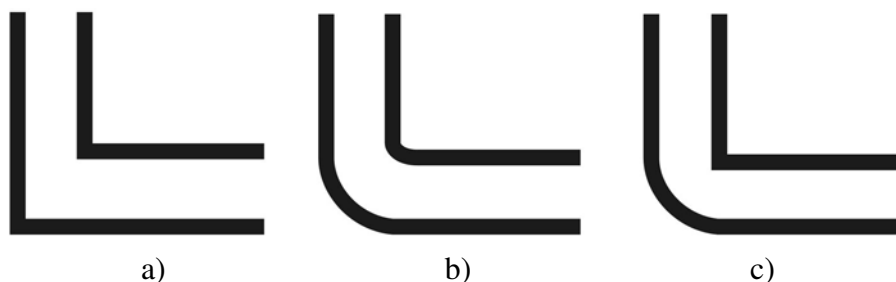


Fig. 5. The most widely used variants of the inner and outer corner shapes

It was necessary to create two different element groups because two kind of material was used. The first material represents material used for the die and plunger. These parts was modeled with the isotropic linear elastic material with the Young’s modulus  $E$  and the Poisson’s

ratio  $\nu$  equal to 210 000 MPa and 0,3 respectively. The second material represents workpiece. The material model with isotropic hardening and diagram of true stress strain behaviour was used. The workpiece material used in the calculations was pure Al, which exhibits strain-rate sensitivity of flow stress and strain-hardening behaviour. The stress-strain curve used for the multilinear elastic-plastic material model was obtained from tensile and compression experimental tests. These obtained values were direct input data for this material model. In this material model was considered with the Young's modulus  $E$  and the Poisson's ratio  $\nu$  equal to 72 000 MPa and 0,3 respectively.

## 5. Obtained results

In the first variant both inner and outer corners are sharp. This combination is shown in fig. 6 and provides that the accumulative effective plastic strains are very high in comparison to the other variants. Main disadvantages of this variant are expensiveness of dies and frequent exchanges of dies because inner sharp corner is usually worn-out very rapidly.

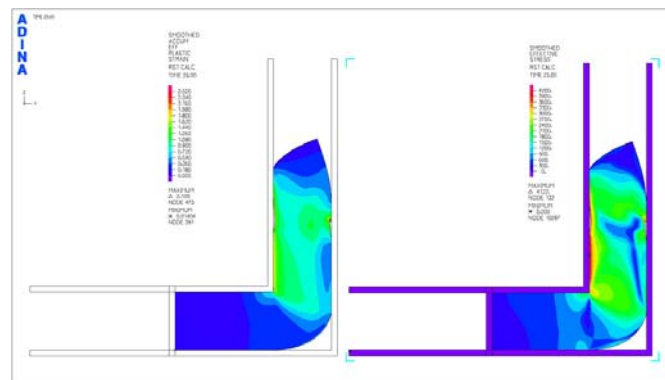


Fig. 6. Distribution of the effective stress and accumulative effective plastic strain in the workpiece during the ECAP process –  $t = 25$  [s] – variant with both sharp corners

In the second variant both inner and outer corners have rounded shape. This variant represents fig. 7. Obtained values of the accumulative effective plastic strain are much lower than in the previous variant. In practice despite of this fact the variant with both round corners is the most widely used. The inner round corner has usually very small radius. Main advantage of this variant is that no empty are made in contrast to the first variant.

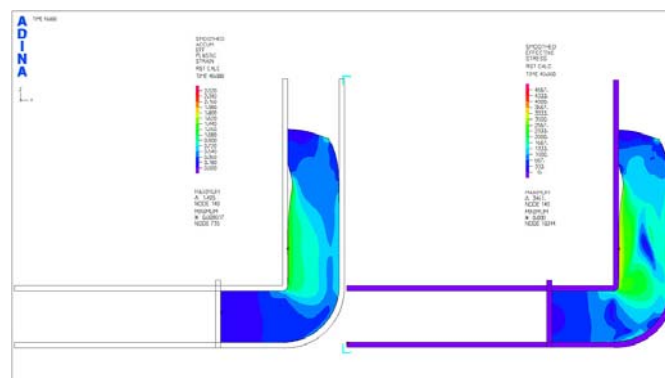


Fig. 7. Distribution of the effective stress and accumulative effective plastic strain in the workpiece during the ECAP process –  $t = 40$  [s] – variant with both round corners.

Fig. 8 shows variant where inner corner is sharp and outer corner has round shape. This variant is combination of the first two above-mentioned variants. Acquired values of effective stress and accumulative effective plastic strain are lower than in the first variant but are higher than in the second variant.

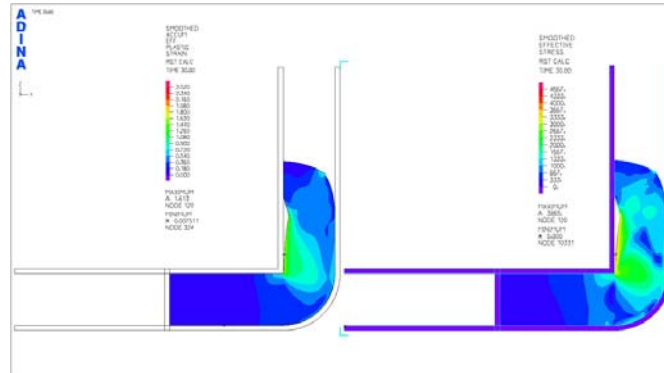


Fig. 8. Distribution of the effective stress and accumulative effective plastic strain in the workpiece during the ECAP process –  $t = 30$  [s] – variant with sharp/round corners

There are presented histograms (see fig. 9) for each analyzed point of interest. Points which lies in the vicinity of the inner side of die and in the front of the workpiece especially point 1 gave inaccurate results. This is valid mainly for the first two variants – in both is presence of the sharp inner corner.

Obtained results of the accumulative effective plastic strain presented above in histograms can lead to expected conclusions. If it takes only points situated out of problematic zones (front part of workpiece and points lies in the vicinity of the inner side of die) thus can be noted that the highest values are obtained from the first variant with both sharp corners.

For passing the workpiece through the die it is necessary to know the pressing force because when it is used the high pressing force the tool of ECAP device can be damaged. Fig. 10 shows the pressing forces acting on the workpiece during ECAP process in analyzed variants.

## 6. Conclusion

It was necessary to analyze behaviour of the accumulative effective plastic strain and effective stress in different region of the aluminium workpiece. Another important data with respect to safe operation mode of pressing device is pressing force acting on the plunger and workpiece, respectively.

FEM analysis of deformation behaviour during ECAP process showed the tremendous increase of plastic deformation. This fact can be easily seen from the histograms of the accumulative effective plastic strain. From obtained results can be seen that only in the points situated in the edge of workpiece passing over the inner die (top side of workpiece) occur higher straining than in the rest of workpiece. This fact is valid for all carried out simulations.

Both the largest and uniform accumulative effective plastic strain increased with the decrease of the radius of the corner die.

The force required to press the workpiece through the die decreased with the increase in the radius of the corner die. This fact can be easily seen from the courses of pressing forces in the fig. 10. The courses are similar but obtained values are different. The first variant with

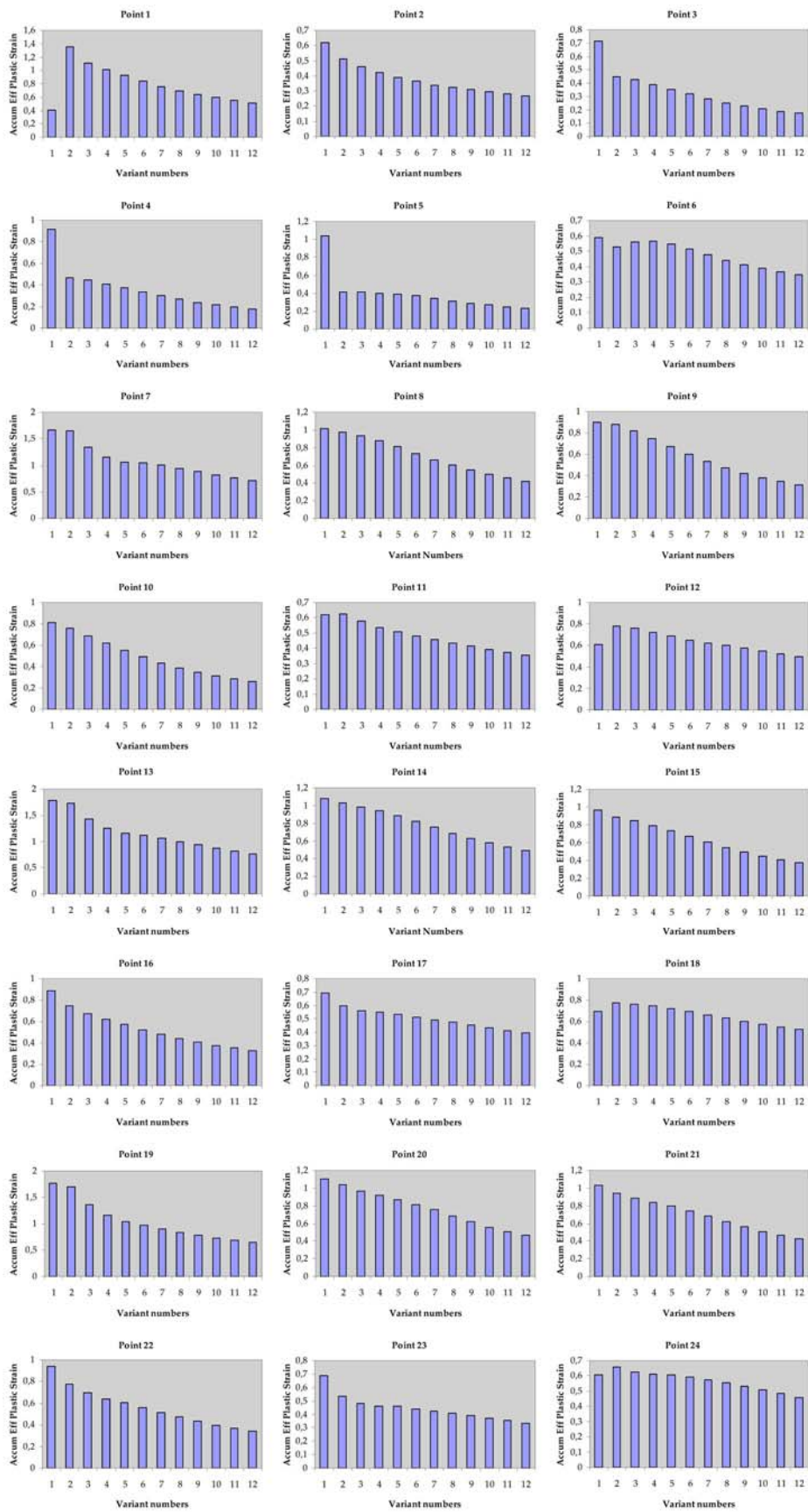


Fig. 9. Comparison of values of accumulative effective plastic strain in all 24 points in m01–m12

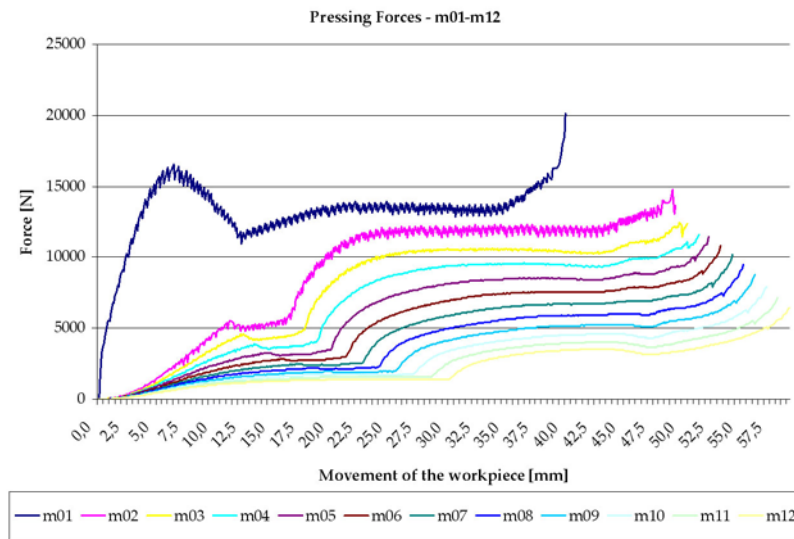


Fig. 10. Pressing forces acting on the workpiece in used variants m01–m12

both sharp corners needs the highest pressing force in the first stage of pressing. This fact fully satisfied the general assumption.

The precision of obtained results can be influenced by contact and its weak formulation. Another fact that can influence the results may be the discretization of solution on the finite elements.

### Acknowledgements

The work has been supported by the grant projects KEGA 3/5028/07 and VEGA 1/0125/09.

### References

- [1] Melicher, R., Numerical simulation of bulk nanostructured materials processed by the method of equal channel angular pressing, Ph. D. thesis, Žilinská univerzita, Strojnícka fakulta, Žilina 2008.
- [2] Melicher, R., Handrik, M., Analysis of shape parameters of tool for ECAP technology, *Acta Mechanica Slovaca* 3-C/2008, Košice, 2008, pp. 273–284. (in Slovak)
- [3] Melicher, R., Finite element method simulation of equal channel angular pressing, In *Transcom 2009*, Žilina, 2009, p. 91–94.
- [4] Melicher, R., Finite element analysis of plastic deformation of aluminium specimen by ECAP process. In *Nekonvenčné technológie 2008*, 21/235, p. 1–12. (in Slovak)
- [5] Melicher, R., Mechanical modeling of severe plastic deformation by ECAP and ECAR technology, *Písomná časť dizertačnej práce*, Žilinská univerzita, Strojnícka fakulta, Žilina 2007. (in Slovak)